Pulse shaping by the electro-optic effect in chirped periodically poled lithium niobate

Rongan Huang, Xianfeng Chen, Jianhong Shi, and Yuxing Xia

We propose an ultrafast pulse shaping method by modulating the pulse phase and amplitude by the electro-optic effect and Bragg diffraction in the aperiodically optical superlattice. Linear-chirped periodically poled lithium niobate is used. The input pulse can be shaped, for example, by compressing it through the extraordinary refractive index change of the crystal by applying and changing the external electric field. © 2007 Optical Society of America

OCIS codes: 320.5520, 140.7090, 230.2090, 050.1940.

1. Introduction

Since the reliable generation of ultrafast pulses below 100 fs in duration occurred for the first time in the 1980s, the topic of femtosecond pulse shaping came into being very soon thereafter and has attracted more and more attention and interest. Ultrafast pulse shaping can be operated in both the time and frequency domains. Unfortunately, modulators are too slow with time modulation. Currently, the main method is to frequency disperse or Fourier transform the pulse in space and modulate the spectrum and spectral phase by creating a spatially varying transmission and phase delay. Over the past decade, powerful pulse shaping methods based on frequency modulation have been developed, such as liquid-crystal arrays,[1,2] deformable mirrors,[3] and acousto-optic modulators (AOMs).[4,5] These optical waveform synthesis methods allow generation of complicated ultrafast optical waveforms according to different user specifications.

Among these modulators, the AOM is a relatively mature technology that has been commercially available for many years. In the AOM, an acousto-optic crystal, typically TeO_2, is driven by a shaped rf voltage signal, which creates a traveling acoustic wave by a piezoelectric transducer. The acoustic wave propagates through the crystal with velocity v_{ac}, causing the formation of a refractive index grating through the photoelastic effect. The grating period Λ is given by v_{ac}/ν, where ν is the rf drive frequency. The grating can be phase, amplitude, or frequency modulated through the use of a correspondingly modulated rf drive waveform, which leads to different Λ at different ν. When the spatially dispersed optical frequency components diffract off the grating, the optical spectrum is modified according to the grating spatial modulation function. It results in the desired Fourier transform pulse shaping operation.[6]

Similar to the AOM, an aperiodically optical superlattice, such as aperiodically poled lithium niobate, is also capable of pulse modulation, which has been studied in the field of nonlinear optical interactions because of its effective laser frequency conversion. In an optical superlattice, spontaneous polarization is periodically or aperiodically reversed by domain inversion. Besides the nonlinear optical coefficient, other third-rank tensors, such as the electro-optic (EO) coefficient, are also modulated. Bragg grating devices based on periodically poled lithium niobate (PPLN) can be used as an optical filter or switch and were introduced by Yamada *et al.*[7] and Gnewuch *et al.*[8] using visible light at 633 nm as a switch with one input and six outputs. The light of some wavelengths that satisfies the Bragg relation can be deflected from the original direction when passing through the PPLN.

In this paper, we propose a new kind of pulse shaping method by employing linear-chirped PPLN. Compared with the traditional pulse shaping method, it takes advantage of one-chip integration in lithium niobate and can be tuned by EO effects. The pulse

The authors are with the Department of Physics, State Key Laboratory on Fiber Optic Local Area Communication Networks and Advanced Optical Communications Systems, Shanghai Jiao Tong University, 800 Dong Chuan Road, Shanghai 200240, China. X. Chen's e-mail address is xfchen@sjtu.edu.cn.

Received 24 July 2006; revised 15 September 2006; accepted 26 September 2006; posted 27 September 2006 (Doc. ID 73349); published 25 January 2007.

0003-6935/07/050795-05$15.00/0

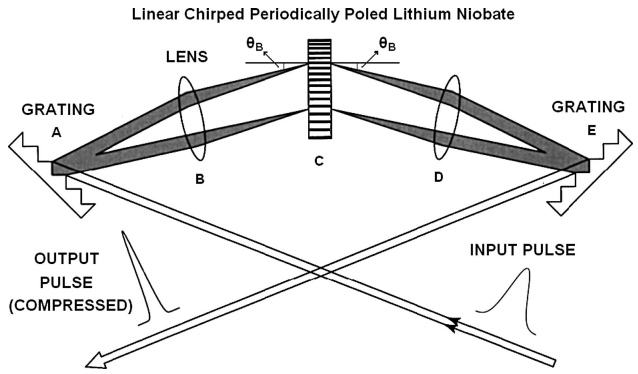

Fig. 1. Pulse shaping apparatus based on the linear-chirped PPLN crystal.

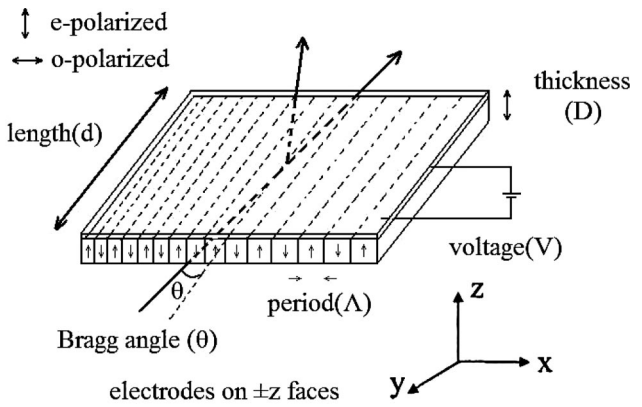

Fig. 2. Schematic of a linear-chirped PPLN pulse modulator device.

shaping method we proposed is similar to the AOM in which the acousto-optic crystal is replaced by a domain-inverted linear-chirped PPLN. The apparatus is depicted in Fig. 1.

As shown in Fig. 1, A, E and B, D represent a pair of diffraction gratings and lenses, arranged in a configuration known as a zero dispersion pulse compressor. The first lens performs a Fourier transform that converts the angular dispersion from the grating to a spatial separation at the back focal plane before the input pulse reaches the $LiNbO_3$. The $LiNbO_3$ is linear chirped periodically poled, shown as C, which means the periods in the crystal are changing gradually from one side to the other. If we apply an external electric field along the c axis of the crystal, a Bragg-diffraction grating with gradually changing period Λ will be formed in the crystal. An optical pulse of a different wavelength will diffract off the grating in the same direction of Bragg angle θ_B at the corresponding point of period Λ. Meanwhile, the pulse phase and amplitude can be modulated because of the difference in refractive indices between the adjoining domains, which are controlled rapidly by varying the amplitude of the applied external electric field. After that, the second lens and grating recombine all the frequencies into a single collimated beam and the shaped output pulse is obtained.

2. Modeling

In this section a theoretical analysis is discussed to obtain useful equations for designing an ultrafast pulse modulator that is composed of a lithium niobate crystal with linear-chirped periodically inverted domains and electrodes on both faces of the crystal. The area of periodically domain-inverted regions form a grating of length d and thickness D as shown in Fig. 2.

By applying an external electric field E, the extraordinary refractive index change of lithium niobate crystal caused by the EO effect is shown in the following equation:

$$\Delta n_e(\lambda, E) = \frac{1}{2}[n_e(\lambda)]^3 r_{33} E, \tag{1}$$

where r_{33} is a tensor element of an EO effect with a value for a lithium niobate crystal of about 30.8×10^{-12} mV.

The incident light of the input pulse with a polarization parallel to the c axis of the crystal that propagates through the crystal between both electrodes on both faces of the crystal is diffracted by the Bragg-diffraction grating induced by the voltage applied between the electrodes. The Bragg angle is described as

$$\sin \theta_B = \frac{\lambda}{2n_e\Lambda}, \tag{2}$$

where θ_B is the incident Bragg angle, and n_e is the extraordinary refractive index of lithium niobate crystal, which is given by the Sellmaier equation[9]:

$$n_e^2(\lambda, T) = A + \frac{B_1}{\lambda^2 - B_2^2} - C_1 \quad (\lambda; \mu\text{m}), \tag{3}$$

where A, B_1, B_2, and C_1 are $4.5567 + 2.605 \times 10^{-7}T^2$, $0.0970 + 2.70 \times 10^{-8}T^2$, $0.201 + 5.4 \times 10^{-8}T^2$, and 0.0224, respectively. T is the temperature of a lithium niobate crystal measured in degrees Kelvin, and n_e is the function of wavelength λ and temperature T.

From Eqs. (2) and (3), if we determine the incident Bragg angle θ_B and temperature T, we can see that the period Λ is only related to the wavelength λ, which is shown in Eq. (4):

$$\Lambda = \frac{\lambda}{2n_e \sin \theta_B}. \tag{4}$$

Using Eq. (4), we can determine the period distribution in the crystal to allow the entire incident light with different wavelength λ to meet the Bragg condition. After we spatially disperse the input pulse, λ changes linearly up to down and so does the value of Λ, just like a linear chirp, which is shown clearly in Fig. 1. The arrangement and parameters of the gratings and lens employed in the following cal-

culations are from the AOM pulse shaping method.[4] The grating's density is $1/d = 1800$ lines/mm and the lens's focus is $F = 30$ cm. According to this configuration, we first calculate the spectral distribution, and then the chirped PPLN is designed and arranged so that input pulses with different wavelengths can be launched to the corresponding point of period in the crystal.

According to Eq. (1), the phase shift $\Delta\phi(\lambda, E)$ given to the light passing through the length L in the crystal is shown as follows:

$$\Delta\phi(\lambda, E) = \frac{2\pi}{\lambda}\Delta n_e(\lambda, T, E)L. \tag{5}$$

Because the incident Bragg angle θ_B is very small (about 0.5°), the length L is nearly the same as the whole length of the crystal d. Therefore it is suitable for us to replace L with d. From Eqs. (1) and (5), the phase modulation equation is given as

$$\Delta\phi(\lambda, E) = \frac{\pi}{\lambda}[n_e(\lambda, T)]^3 r_{33}\frac{V}{D}d, \tag{6}$$

where V is the applied voltage between the electrodes, and D is the thickness of the lithium niobate crystal, which is shown in Fig. 2.

Equations (3) and (6) show that two approaches can be employed to modulate the phase: temperature and applied voltage. When temperature is fixed and we apply different voltages at different points of period Λ on the crystal, the phase of the pulse component of corresponding wavelength can be changed as we desire. On the other hand, if we apply a uniform voltage between the two electrodes of the linear-chirped PPLN crystal and linearly changing temperature over the crystal, the value of n_e will also distribute linearly, which leads to the same effect of phase modulation of the corresponding wavelength.

While the phase modulation is operating, the first-order diffraction efficiency of such a thick Bragg grating is given by the equation[9,10]

$$\eta = \sin^2\left(\frac{\pi d}{2\lambda}[n_e(\lambda)]^3 r_{33}\frac{V}{D}\right). \tag{7}$$

This efficiency equation only holds when the Bragg relation [Eq. (2)] is satisfied. It is possible to design a device that could give high theoretical diffraction efficiencies at any given wavelength. As shown in Eqs. (6) and (7), when the voltages are applied, the modulation of the phase and amplitude interact with each other. This also often occurs in other methods of pulse shaping, such as use of AOMs and liquid-crystal spatial light modulators (SLMs). This problem makes the pulse shaping more complex. In general, if the input pulse is known and the output is targeted, the direct calculation of $H(\omega)$ requires both a phase and an amplitude mask, as shown in Eq. (8):

$$H(\omega) = \frac{\tilde{E}_{out}(\omega)}{\tilde{E}_{in}(\omega)}. \tag{8}$$

In the field of pulse shaping, the spectral phase is more important than the amplitude for determining $E(t)$; therefore, we should calculate the best possible phase-only mask. Some optimization algorithms have been proposed to deal with such problems.

3. Theoretical Simulation in Pulse Compression

Pulse compression is one of the most common aspects in the field of pulse shaping. The periods of the crystal are calculated according to Eq. (2) with the wavelength from 795 to 815 nm. The calculation result is shown in Fig. 3 as an example of the period and corresponding wavelength.

To generate a compressed pulse, the phase modulation is much more important than the amplitude modulation, for which we are able to use Eq. (6) to calculate the phase modulation instead of the optimization algorithms mentioned above.

In pulse compression, the desired waveform is

$$E_{out}(\Omega) = \frac{1}{\sqrt{2\pi}}E_0\tau_0\exp\left[-\frac{1}{2}\tau_0^2\Omega^2\right], \tag{9}$$

where $\Omega = \omega - \omega_0$, E_0 is the initial amplitude of the pulse, and τ_0 is the field HWHM. It is clear that the phase for different frequencies of the compressed pulse is all the same or equal to zero [$\phi_{out}(\omega) = 0$].

Generally, we suppose that the input pulse is the chirped Guassian pulse:

$$E_{in}(\Omega) = \frac{1}{\sqrt{2\pi}}E_0\tau_0\exp\left[-\frac{1}{2}(\tau_0^2 + iC_1)\Omega^2\right], \tag{10}$$

where C_1 is related to the duration time of the pulse and $C_1 = 4\tau_0^2$ ($\tau_0 = 40$ fs), so the initial phase of the

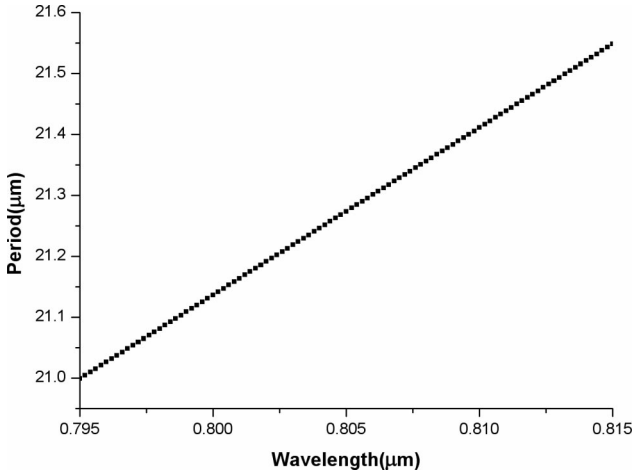

Fig. 3. Calculated result of a relation between the periods in the crystal and the corresponding wavelengths of the incident pulse.

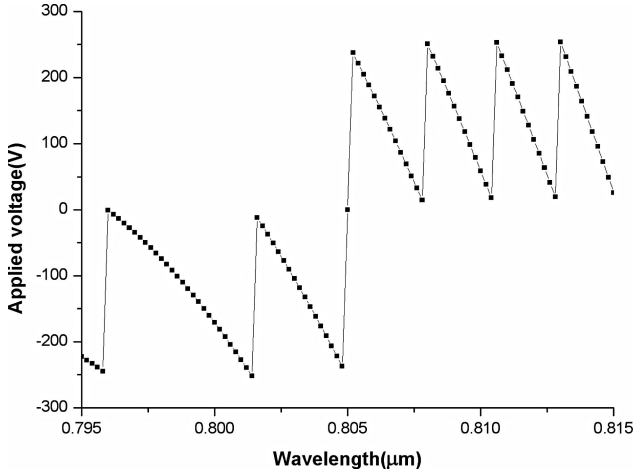

Fig. 4. Calculated result of a relation between the values of applied voltage on the lithium niobate crystal and the corresponding wavelengths of the incident pulse.

input pulse is shown as follows:

$$\phi_{in}(\omega) = -\frac{1}{2} C_1 \Omega^2 = -\frac{1}{2} C_1 (\omega - \omega_0)^2. \qquad (11)$$

The length of the crystal is 10 mm and the thickness is 0.5 mm. Considering the pulse transmission path and the phase modulation equation (6), we can calculate the modulation voltage, which is shown in Fig. 4.

Meanwhile, the amplitude of the input pulse is also modulated by the applied voltages. The result is shown in Fig. 5. Some near-zero-amplitude points are observed because the corresponding applied voltages are shifted sharply, which leads to the loss of some frequency spectra of the input pulse. This phenomenon is similar to the dead spaces in a liquid-crystal SLM.

When the external field is applied on the sample, the index n_e will be changed due to the EO effect.

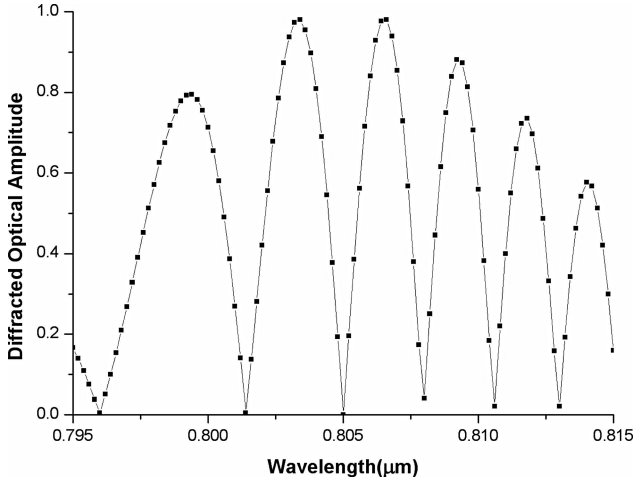

Fig. 5. Calculated result of a dependence of a diffracted optical power of different wavelengths of the input pulse on the applied voltages between the electrodes on both faces of the crystal.

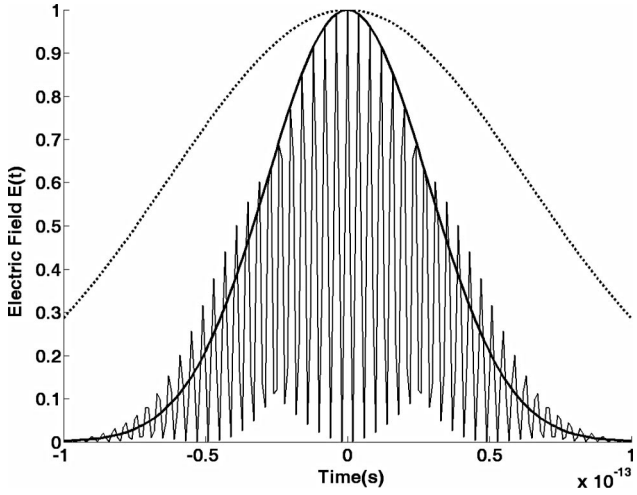

Fig. 6. Calculated result of pulse compression (790–820 nm). x axis, time; y axis, electric field of the optic pulse. Dotted curve, electric field of the input chirped Guassian pulse; solid curve, compression limit decided by $\Delta\nu\Delta t \approx 1$. Oscillation curve, calculation result of the output pulse.

From Eq. (4), the change of Bragg angle can be calculated as small as $\Delta\theta_B = (1.85 \times 10^{-5})°$ when the maximal voltage 253.5 V is applied at the wavelength of $\lambda = 813$ nm. According to Eq. (7) in Ref. 9, the actual diffracted light power ratio at the optical incident angle for 813 nm is calculated as 0.999978 compared to the unit diffracted light power ratio when there is no external E field applied. Therefore the change of the electric field applied on the modulator has minimal influence on the propagation of the spectrum through the modulator.

The pulse shaping result is shown in Fig. 6. The input chirped Guassian pulse (dotted curve), the compression limit ($\Delta\nu\Delta t \approx 1$, solid curve) and the calculated output pulse (oscillation curve) are shown in the graphs. It is obvious that the calculated output pulse in Fig. 6 is well compressed, which is close to the transform limit. The spectrum range in our simulations is from 790 to 820 nm, totaling 151 sample points.

4. Conclusion

In this paper, we have investigated a new, to our knowledge, pulse shaping method with linear-chirped periodically poled lithium niobate. The Bragg-diffraction and the linear distributed periods in the lithium niobate allow the input pulse with all different wavelengths to diffract in the same direction of the Bragg angle θ_B. Meanwhile, the phase and amplitude of the input pulse can be modulated through the extraordinary refractive index change of lithium niobate crystal caused by the EO effect when the external voltage is applied and changed. As an example, we have demonstrated the theoretical calculation result of the pulse compression by means of this pulse shaping method. Compared to the AOM method, the pulse shaping method based on Bragg diffraction and the EO effect has the advantages of lower external

drive voltages and faster response times. Experimental demonstration and more theoretical calculations, such as optimization algorithms for the shaping of square pulses and pulse trains, are in progress.

This research was supported by the National Natural Science Foundation of China (projects 60477016 and 10574092), the Foundation for Development of Science and Technology of Shanghai (project 04DZ14001), and the Shu-Guang Scholar Plan of the Shanghai Education Committee.

References

1. D. Yelin, D. Meshulach, and Y. Silberberg, "Adaptive femtosecond pulse compression," Opt. Lett. **22,** 1793–1795 (1997).
2. A. Efimov, M. D. Moores, N. M. Beach, J. L. Krause, and D. H. Reitze, "Adaptive control of pulse phase in a chirped-pulse amplifier," Opt. Lett. **23,** 1915–1917 (1998).
3. E. Zeek, K. Maginnis, S. Backus, U. Russek, M. Murnane, G. Mourou, H. Kapteyn, and G. Vdovin, "Pulse compression by use of deformable mirrors," Opt. Lett. **24,** 493–495 (1999).
4. M. A. Dugan, J. X. Tull, and W. S. Warren, "High-resolution acousto-optic shaping of unamplified and amplified femtosecond laser pulses," J. Opt. Soc. Am. B **14,** 2348–2358 (1997).
5. M. R. Fetterman, D. Goswami, D. Keusters, W. Yang, J.-K. Rhee, and W. S. Warren, "Ultrafast pulse shaping: amplification and characterization," Opt. Express **3,** 366–375 (1998).
6. A. M. Weiner, "Femtosecond pulse shaping using spatial light modulators," Rev. Sci. Instrum. **71,** 1929–1960 (2000).
7. M. Yamada, M. Saitoh, and H. Ooki, "Electric-field induced cylindrical lens, switching and deflection devices composed of the inverted domains in LiNbO3 crystals," Appl. Phys. Lett. **69,** 3659–3661 (1996).
8. H. Gnewuch, C. N. Pannell, G. W. Ross, P. G. R. Smith, and H. Geiger, "Nanosecond response of Bragg deflectors in periodically poled $LiNbO_3$," IEEE Photon. Technol. Lett. **10,** 1730–1732 (1998).
9. M. Yamada, "Electrically induced Bragg-diffraction grating composed of periodically inverted domains in lithium niobate crystals and its application devices," Rev. Sci. Instrum. **71,** 4010–4016 (2000).
10. J. A. Abernethy, C. B. E. Gawith, R. W. Eason, and P. G. R. Smith, "Demonstration and optical characteristics of electro-optic Bragg modulators in periodically poled lithium niobate in the near-infrared," Appl. Phys. Lett. **81,** 2514–2516 (2002).